

# Chapter 8

## Graphene-TiO<sub>2</sub> Photocatalyst for Efficient Sunlight-Driven Degradation of Methyl Orange

K. Alamelu and B.M. Jaffar Ali

**Abstract** In this study, graphene-TiO<sub>2</sub> nanocomposites at varying composition of graphene oxide were prepared following hydrothermal method. In order to optimize the composition and time of degradation, photocatalytic efficiency was studied for the composition range 1–10 wt% of graphene oxide. The nanocomposites exhibited good visible light photocatalytic activity for the degradation of Methyl Orange in all the composition range studied. The 10 wt% graphene-TiO<sub>2</sub> found to exhibit photocatalytic degradation of 98% Methyl Orange in 75 min which was 2.5 fold higher than pristine TiO<sub>2</sub> nanoparticles. The band gap of the composites were found to decrease continuously from 3.0 to 2.5 eV, indicating marked red-shift in absorbance spectrum with increased graphene oxide. The enhanced photocatalytic efficiency of composite in comparison to pristine TiO<sub>2</sub> demonstrates corresponding visible light active nature of photocatalysis. We attribute this to the synergetic effect of reduced the electron-hole pairs recombination enabled by graphene oxide intercalation, increased surface area, and creation of more reaction active sites.

**Keywords** Graphene oxide · TiO<sub>2</sub> · Methyl orange · Hydrothermal synthesis · Photocatalytic activity

### 8.1 Introduction

TiO<sub>2</sub> is one of the most studied semiconducting materials, that exhibit excellent photocatalytic activity and is used in wide range of application [1]. However, the photocatalytic efficiency of the TiO<sub>2</sub> is limited due to the larger band gap (~3.2 eV) of the material, faster electron-hole recombination and its absorption only in the UV range. Many methods were investigated to increase the performance of TiO<sub>2</sub> using metal, non-metal doping and carbon based composites materials [2].

---

K. Alamelu · B.M. Jaffar Ali (✉)  
Centre for Green Energy Technology,  
Pondicherry University, RV Nagar, Kalapet 605014, Pondicherry, India  
e-mail: jaffarali.bm@gmail.com

Graphene, an inexpensive, two dimensional sp<sup>2</sup>-hybridized novel carbonaceous material, has attracted much attention because of its unique properties such as high surface area ( $\sim 2600 \text{ m}^2/\text{g}$ ), electron mobility ( $\sim 15,000 \text{ m}^2/\text{V.s}$ ) of charge carriers, chemical stability, optical transparency and mechanical strength [3]. In Graphene based composites, graphene acts as an ideal electron acceptor and good electron transporting bridge due to its high electron mobility and conjugation structure [4]. Carbon materials have astonishing adsorption properties therefore mainly used in various environmental applications.

## 8.2 Experimental Section

### 8.2.1 Reagents and Material

Graphite flakes, n-propanol, titanium tetraisopropoxide, Sodium nitrate, potassium permanganate purchased from Spectrochem. Hydrogen peroxide (30%), sulphuric acid, nitric acid, hydrochloric acid, ethanol and Methyl Orange from Merck were used as received.

### 8.2.2 Synthesis of $\text{TiO}_2$

$\text{TiO}_2$  nanoparticles were synthesized by hydrothermal method. Titanium tetra isopropoxide was dissolved in n- propanol to form solution. The diluted nitric acid (0.65 M) was added to the above solution magnetic stirred for 1 h to form clear solution. The transparent solution was transferred into a Teflon lined stainless steel autoclave and heated to 175 °C and maintained for 12 h. After cooling into room temperature the formed precipitates were separated by centrifugation, washed twice with distilled water and then dried at 80 °C for 24 h. The dried powder was calcinated at 400 °C for 3 h.

### 8.2.3 Synthesis of Graphene- $\text{TiO}_2$ Nanocomposites

Graphene oxide was synthesized by the modified Hummer's method. Different weight percentages (1, 3, 5, 7 and 10 wt%) of grapheneoxide- $\text{TiO}_2$  composites was prepared following hydrothermal method. Graphene Oxide was dissolved in mixture of water and ethanol ultrasonic treatment for 1 h. Prepared  $\text{TiO}_2$  was added to the obtained GO solution and stirred for 2 h, to get a homogeneous suspension. The suspension was placed in a 200 mL Teflon lined stainless steel autoclave and heated to 120 °C for 24 h, to achieve reduction of GO to graphene sheets and the deposition of  $\text{TiO}_2$  over the graphene sheets. The resulting composite was recovered by centrifugation and washed copiously with DI water, and dried at 70 °C for 12 h.

### 8.2.4 Characterization

The crystal structure and phase composition of the synthesized photocatalysts was examined by X-ray diffractometer (XRD, Rigaku, Ultima IV, Tokyo, Japan) operated in the reflection mode with Cu K $\alpha$  radiation ( $\lambda = 1.5406 \text{ \AA}$ ). UV-vis diffuse reflectance spectra (UV-DRS) were measured using UV-vis spectrophotometer (Lambda 650 Perkin Elmer Spectrometer) equipped with an integrating sphere attachment. The spectra were collected with BaSO<sub>4</sub> as a reference. A confocal micro-Raman spectrometer with a laser beam of 514 nm (Renishaw, Model: RM 2000) was used to identify the properties of carbonaceous materials. Photoluminescence spectra (PL) were recorded using Spectrofluorometer with the 325 nm excitation (Jobin Yvon, Model: Fluorolog-FL3-11). Dye degradation profile has been studied using custom configured Ocean Optics spectrophotometer with LS1 light source, USB 2000 detector and Spectrasuite data acquisition system.

### 8.2.5 Photocatalytic Experiment

The photocatalytic activities were determined based upon the removal of Methyl Orange in aqueous solutions. For photocatalytic reaction, 0.5 mg/mL photocatalyst was suspended in the aqueous solution of the Methyl Orange (0.02 mM), magnetically stirred in dark condition for 45 min to attain adsorption-desorption equilibrium. For the photocatalytic degradation experiment the photocatalytic reaction was initiated by exposure of direct sunlight and then 2 mL of sample was drawn at 15 min interval. The suspended photocatalyst was removed by centrifugation, and the resulting solution analysed with the UV-Visible spectrometer by recording the absorption band maximum of Methyl Orange.

## 8.3 Results and Discussion

The crystallographic structures and phase composition of the materials were characterized by X-ray diffraction. Figure 8.1 shows the XRD pattern of TiO<sub>2</sub> and different weight percentage of graphene-TiO<sub>2</sub> composites. The XRD pattern of GO exhibits major peak at 11.12 corresponds to (002) plane with d-spacing value of 0.795 nm, which is much higher than d-spacing value of graphite, which indicates the oxidation of graphite to graphene oxide (GO) [5]. Diffraction pattern of TiO<sub>2</sub> shows the major peaks around the  $2\theta$  values 25.3 and 27.5 corresponding to anatase (101) and rutile (110) phases respectively which confirms the biphasic nature of the synthesized materials.

As TiO<sub>2</sub> nanoparticles have great absorption in the ultraviolet region, we find that introduction of graphene sheets shifts absorption edge of the nanocomposites

**Fig. 8.1** X-ray diffraction pattern of GO, TiO<sub>2</sub> and (1–10 wt%) G-TiO<sub>2</sub> composites

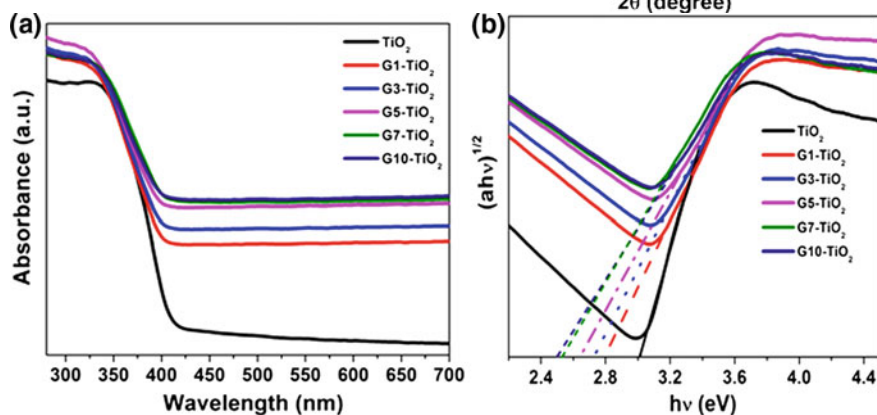
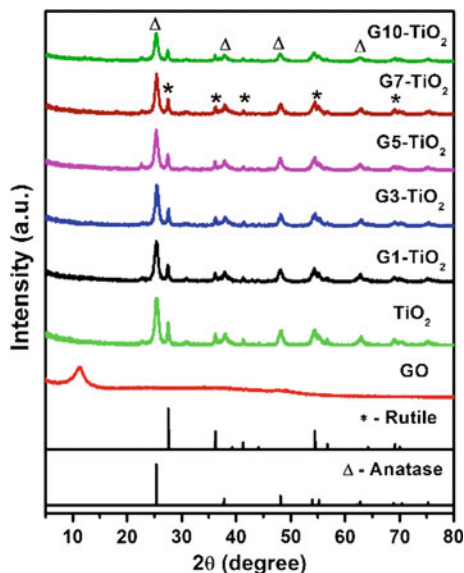


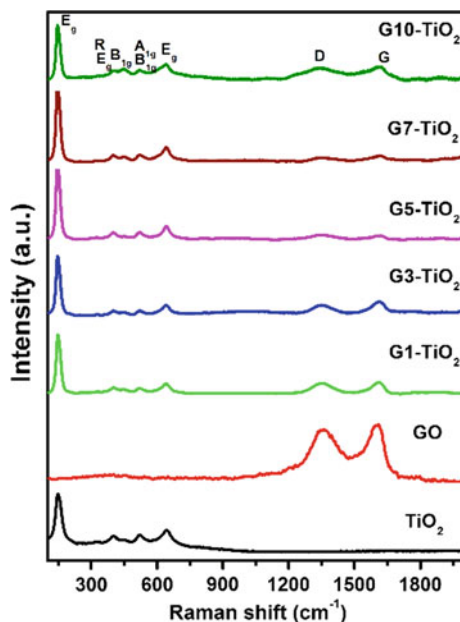
**Fig. 8.2** **a** UV-DRS spectra of TiO<sub>2</sub> and (1–10 wt%) G-TiO<sub>2</sub> composites, **b** Tauc plot of TiO<sub>2</sub> and (1–10 wt%) G-TiO<sub>2</sub> composites

towards the visible region. In order to estimate the bandgap of the materials, a tauc plot is generated from transformed Kubelka-Munk function as a function of energy of light shown in Fig. 8.2b and bandgap values deduced. Table 8.1 gives the bandgap of graphene-TiO<sub>2</sub> composites for varying composition (1–10 wt%) of graphene. It is observed that increasing weight percentage of graphene resulted in decreasing bandgap (Fig. 8.3).

The Raman spectrum of GO shows D- and G- bands at  $\sim 1354$  and  $\sim 1617$  cm<sup>-1</sup>, respectively. The peak intensity ratio  $I_D/I_G$  for GO was found to be 0.91. The Raman spectrum of the TiO<sub>2</sub> and (1–10 wt%) G-TiO<sub>2</sub> exhibit peaks at 147.3, 401, 520.5 and 638 cm<sup>-1</sup>, which were assigned to Eg, B1g, A1g + B1g and

**Table 8.1** Bandgap values of TiO<sub>2</sub> and (1–10 wt%) G-TiO<sub>2</sub> composites

S. no	Samples	Bandgap (eV)
1	TiO <sub>2</sub>	3.00
2	G1-TiO <sub>2</sub>	2.81
3	G3-TiO <sub>2</sub>	2.73
4	G5-TiO <sub>2</sub>	2.64
5	G7-TiO <sub>2</sub>	2.53
6	G10-TiO <sub>2</sub>	2.50

**Fig. 8.3** Raman spectra of TiO<sub>2</sub> and (1–10 wt%) G-TiO<sub>2</sub> composites

$E_g$  of anatase phase titania. The peaks at  $248\text{ cm}^{-1}$  were attributed to the second order effective ( $E_g$ ) of rutile titania.

The PL emission spectra have been used to investigate the efficiency of the charge carrier transfer and the life time of the photogenerated electron-hole in the semiconductor. Figure 8.4 shows the PL emission spectra of TiO<sub>2</sub>, Graphene-TiO<sub>2</sub> nanocomposites. Among all the samples pristine TiO<sub>2</sub> shows higher intensity. It is observed that introduction of graphene sheets quenches the intensity of the composite material, indicating reduced recombination rate of charge carrier.

#### Photocatalytic activity of TiO<sub>2</sub> and (1–10 wt%) G-TiO<sub>2</sub> nanocomposites

Photocatalytic activity of the samples was monitored by discoloration of Methyl Orange dye under direct sunlight irradiation. The percentage of dye degradation in terms of  $C/C_0$  was reported where,  $C_0$  is the initial concentration of the dye and  $C$  is the temporal concentration at time. Figure 8.5 plots the normalized concentration of

**Fig. 8.4** PL emission spectra of TiO<sub>2</sub> and (1–10 wt%) G-TiO<sub>2</sub> composites

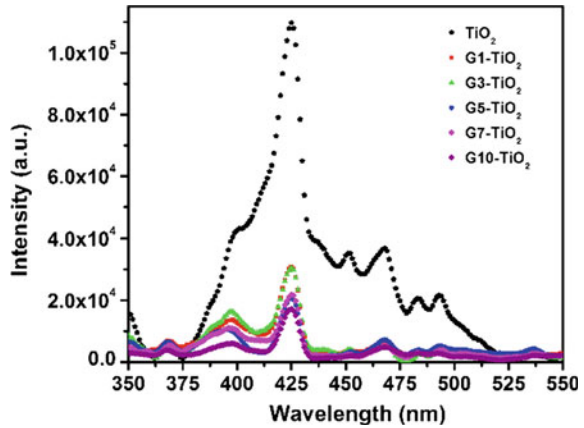
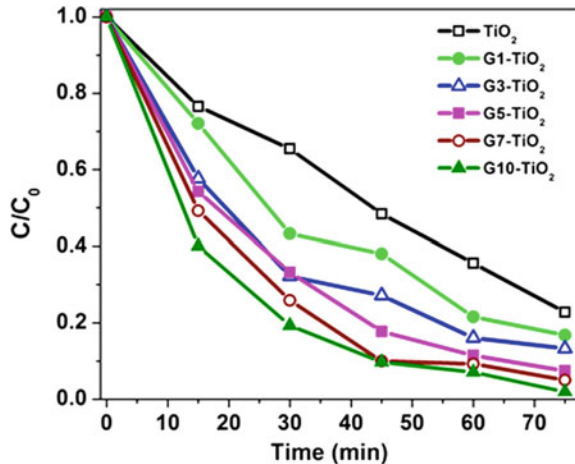


**Fig. 8.5** Change in concentration of MO on TiO<sub>2</sub>, (1–10 wt%) Graphene-TiO<sub>2</sub> nanocomposites under direct sunlight irradiation



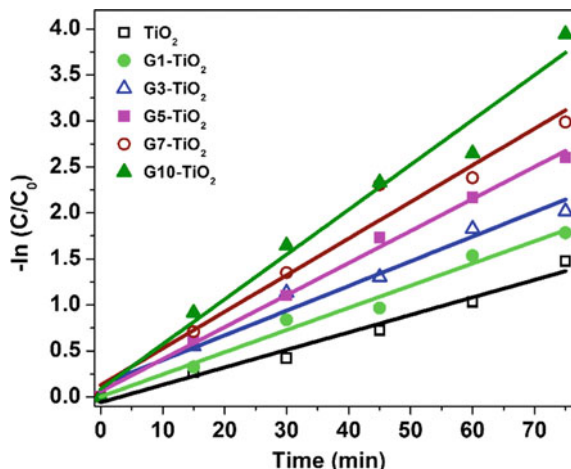
Methyl Orange as a function of time period of photodegradation. Titania nanoparticles degrade about 77% of the dye; with increasing weight percentage of graphene oxide dye degradation percentage increased to 98% within 75 min. Graphene-TiO<sub>2</sub> composite shows excellent photocatalytic activity compare to Pure TiO<sub>2</sub>.

The photocatalytic degradation of the dye was followed pseudo first order kinetics reaction method [6, 7].

$$-\ln\left(\frac{C}{C_0}\right) = kt$$

Where, C<sub>0</sub> is the initial concentration of the dye and C is the temporal concentration at time, k is the rate constant of the reaction, and was determined from a linear fit to the data as shown in Fig. 8.6. The rate constant of the photocatalyst are 0.0190, 0.02413, 0.0268, 0.0348, 0.0398 and 0.0487 min<sup>-1</sup> for TiO<sub>2</sub>, G1-TiO<sub>2</sub>,

**Fig. 8.6** Pseudo-first order kinetics on MO over TiO<sub>2</sub>, (1–10 wt%) Graphene-TiO<sub>2</sub> nanocomposites under direct sunlight irradiation



G3-TiO<sub>2</sub>, G5-TiO<sub>2</sub>, G7-TiO<sub>2</sub> and G10-TiO<sub>2</sub>, respectively. G10-TiO<sub>2</sub> exhibit 2.5 fold higher rate of degradation compare to pristine TiO<sub>2</sub> nanoparticles.

## 8.4 Conclusion

In summary, graphene-TiO<sub>2</sub> composite were prepared by hydrothermal method for varying concentration of graphene oxide. We found that more than 98% of dye solution could be effectively degraded in 75 min by 10 wt% graphene oxide in TiO<sub>2</sub>. The enhanced photocatalytic property is attributed to increased surface area of the composite system due to grapheneoxide-TiO<sub>2</sub> intercalation, the inherent high surface area of graphene oxide sheets that enable higher adsorption of dye, suppressed electron-hole pair recombination and improved charge carrier transport. We found that 10 wt% of Graphene Oxide composite with TiO<sub>2</sub> is therefore optimally suited for removal of organic dye by direct sunlight.

**Acknowledgements** The authors gratefully acknowledge Central Instrumentation Facility (CIF) of Pondicherry University for the instrumentation facilities availed. The author K.A acknowledges the MNRE-National Renewable Energy Fellowship, for their financial support.

## References

1. M.R. Hoffmann, S.T. Martin, W.Y. Choi, D.W. Bahnemann, Environmental applications of semiconductor photocatalysis. *Chem. Rev.* **95**, 69–96 (1995). doi:[10.1021/cr00033a004](https://doi.org/10.1021/cr00033a004)
2. V. Raja, L. Shiamala, K. Alamelu, B.M.J. Ali, A study on the free radical generation and photocatalytic yield in extended surfaces of visible light active TiO<sub>2</sub> compounds. *Sol. Energy Mater. Sol. Cells* **152**, 125–132 (2016). doi:[10.1016/j.solmat.2016.03.008](https://doi.org/10.1016/j.solmat.2016.03.008)

3. Q.J. Xiang, J.G. Yu, M. Jaroniec, Graphene-based semiconductor photocatalysts. *Chem. Soc. Rev.* **41**, 782–796 (2012). doi:[10.1039/C1CS15172J](https://doi.org/10.1039/C1CS15172J)
4. S. Bai, X.P. Shen, Graphene–inorganic nanocomposites. *RSC Adv.* **2**, 64–98 (2012). doi:[10.1039/C1RA00260K](https://doi.org/10.1039/C1RA00260K)
5. N.I. Kovtyukhova, P.J. Ollivier, B.R. Martin, T.E. Mallouk, S.A. Chizhik, E.V. Buzaneva, A. D. Gorchinskiy, Layer-by-layer assembly of ultrathin composite films from micron-sized graphite oxide sheets and polycations. *Chem. Mater.* **11**, 771–778 (1999). doi:[10.1021/cm981085u](https://doi.org/10.1021/cm981085u)
6. L. Sun, Z.L. Zhao, Y.C. Zhou, L. Liu, Anatase TiO<sub>2</sub> nanocrystals with exposed 001 facets on graphene sheets via molecular grafting for enhanced photocatalytic activity. *Nanoscale* **4**, 613–620 (2012). doi:[10.1039/c1nr11411e](https://doi.org/10.1039/c1nr11411e)
7. N. Yang, *The Preparation of Nano Composites and Their Applications in Solar Energy Conversion* (Nature springer, 2017)